

INFLUENCE OF PRECURSOR MOLAR RATIOS ON THE PHYSICAL PROPERTIES OF NANOCRYSTALLINE Cu_{2-x}S THIN FILMS PREPARED BY CHEMICAL BATH DEPOSITION METHOD

I. S. NAJI^{a*}, U. M. SLEMAN^b

^a*Professor, Physics Dept., College of Science, University of Baghdad*

^b*Master student, Physics Dept., College of Science, University of Baghdad, Baghdad / IRAQ*

The nanocrystalline Cu_{2-x}S films were deposited on glass substrates using chemical bath deposition method at 60°C temperature from aqueous solutions composed of different molar ratio of copper sulfate and thiourea as source of Cu^{+2} , S^{-2} ions respectively, and EDTA as a complex agent. X-ray diffraction studies reveal amorphous structure for all samples with a small peaks, and there is a broad hump between 15° and 35°, and always there is more phases appear in the single pattern. The morphology of the Cu_{2-x}S films were studied by atomic force microscopy which showed uniform surface, without cracks and consists of nanosize particles which are well adhered to the substrate. The optical properties of Cu_{2-x}S films were investigated by UV-Vis spectrophotometer. The band gap of the films ranged from 2.78-3.0 eV with changing the molar ratio. Hall effect measurement showed that these films were p-type and the films with $x=0.25$ and $x=0$ had the best characteristics between the other films.

(Received March 2, 2018; Accepted June 3, 2018)

Keywords: copper sulfide films, Structural properties, Optical properties, CBD method

1. Introduction

Transition metal sulfides have been an innovative field of research due to number of interesting optical, electronic and catalytic properties and applications [1]. One of the transition metal sulfides is copper sulfide (Cu_{2-x}S) which is a p-type semiconducting material belongs to I-VI compound [2]. Its act as acceptor semiconductor material mainly due to that of copper vacancies occurring within the lattice [3], and its variable property exhibition depending upon the stoichiometry, $0 \leq x \leq 1$ [4].

Copper sulphide at room temperature occurs in five stable phases namely, covellite (CuS) in the sulphur-rich region, anilite ($\text{Cu}_{1.75}\text{S}$), digenite ($\text{Cu}_{1.8}\text{S}$), djurleite ($\text{Cu}_{1.95}\text{S}$), and chalcocite (Cu_2S) in the copper-rich region [5]. Other phases that exist include yarowite ($\text{Cu}_{1.12}\text{S}$) and spionkopite ($\text{Cu}_{1.14}\text{S}$) [4]. The structure of chalcocite and djurleite is hexagonal with alternate layers of copper and sulphur ions. The covellite contains 6 formula units in the unit cell with four copper ions tetrahedrally coordinated and two triangular coordinates with a hexagonal crystal structure [5]. Among these phases, CuS (covellite) exhibits metal-like electrical conductivity and it also possesses near-ideal solar control characteristics. Notwithstanding to this, they even show easy current-conduction and charge-transfer mechanism [6].

The band gap of Cu_{2-x}S can be varied in a wider range (1.2-2.5 eV) with stoichiometric composition, making it a highly desirable material for photovoltaic cells. Thin Cu_{2-x}S film maintain transmittance in the infrared, low reflectance (<10%) in the visible, and relatively high reflectance (> 15%) in the near-infrared region, which are ideal characteristics for solar energy adsorption [3,7]. Copper sulphide attract much attention due to their wide range of applications in optical and electrical devices, such as selective radiation filters, gas sensors, photo thermal conversion, electroconductive electrodes, microwave shielding coatings, solar control coatings, dye-sensitized solar cells, potential nanometer-scale switch, high capacity cathode material in

*Corresponding author: moonbb_moonaaa@yahoo.com

lithium secondary batteries [8-10].

Different techniques have been used to deposited CuS thin films, such as spray pyrolysis deposition [11], photochemical deposition [12], pulse laser deposition [13], atomic layer Deposition [14], chemical vapor deposition [15], successive ionic layer adsorption and reaction method [16], electrodeposition method [17], chemical bath deposition [18,19]. Chemical bath deposition method is a promising technique because of its simplicity, inexpensive, a large area of thin film can be deposited with out sophisticated instruments, and the properties of the deposited film can be controlled by proper optimization of the chemical bath and deposition conditions [20].

In the present study, we report the preparation of copper sulfide thin films by chemical bath deposition technique and studied the effect of precursor ratios on the structural, morphological, optical and electrical properties.

2. Experimental procedure

Chemical bath deposition technique was used to deposit copper sulphide thin films on glass substrates of dimensions (76mm X 26mm X 1.35mm) which had been previously washed with mild soap solution and rinsed with distilled water and then the glass slides were immersed in dilute hydrochloric acid for 48hrs. Again the glass slides were washed with de-ionized water and finally ultrasonically cleaned by ethanol then dried in oven for 1hr at 50° C.

The Chemical bath composition was copper sulfate pentahydrate solution ($\text{CuSO}_4 \cdot 5\text{H}_2\text{O}$) and thiourea ($(\text{NH}_2)_2\text{CS}$) as source of Cu^{+2} , S^{-2} ions respectively, with disodium methylene diamine tetraacetate ($\text{Na}_2\text{EDTA} \cdot 2\text{H}_2\text{O}$) as complex agent with Cu^{2+} to obtain Cu-EDTA complex solution. The presence a complex agent EDTA in solution help to improve the lifetime of the deposition bath and adhesion of deposited films on glass substrate. To maintain basic medium, ammonium hydroxide (NH_4OH) was used to adjusting PH of the solution.

The procedure to prepare CuS film involve taking 15 ml copper salt as Cu^{+2} ion source in 100ml beaker, 15 ml of complex agent is mixed drop wise, the solution is stirred constantly for few min for getting homogenous mixture. Then add NH_4OH drop wise until the colour of the solution changes from light blue colour to dark blue colour (pH=10). After this add 15ml thiourea as S^{-2} ion source, stir the solution for 15 min, then the solution colour become olive. Two cleaned slides (face to face) was used and band tightly together by teflon tape in one end, and then immersed vertically in the solution. Keep the reaction mixture in water bath at 60° C, the slides were taken out after 90min. After this time the reaction was completed and the particles settled down at the bottom of the beaker. The slides which were taken out washed with distilled water carefully in good way. The substrate place in air at room temperature until it dried.

Five reaction baths were used trying to obtain different copper sulfide thin films with different phases (CuS , $\text{Cu}_{1.75}\text{S}$, $\text{Cu}_{1.8}\text{S}$, $\text{Cu}_{1.95}\text{S}$ and Cu_2S) by changing Cu/S molar ratio in the solution.

The crystal structure analysis of these films has been examined by using X-ray diffractometer type (Miniflex II Rigaku company, Japan) with CuK_α radiation of wavelength 0.154nm and $2\theta=5^\circ-70^\circ$. The microstructure analysis was investigated by using Atomic force microscope (AFM), model CSPM-AA 3000 contact mode spectrometer, Angstrom Advanced Inc. Company, USA, and the films surface topography with image size (2000 nm, 2000 nm). The optical transmittance of the films was recorded using UV-Visible spectrophotometer type (SP8001 Metertech, USA) over the wavelength range (190-1100) nm. The electrical properties were measured using a Hall Effect measurement System (HMS-3000 VER 3.5) at room temperature.

3. Results and discussion

The structure of Cu_{2-x}S thin films are deposited on a glass substrate by chemical bath deposition with different atomic weight to obtain different x value, as shown in figure (1). The

XRD patterns of all samples show an amorphous structure with a small peaks, there is a broad hump between 15° and 35° is due to the amorphous glass substrate [21].

The XRD pattern of a CuS film (fig.1a) reveals four orientations, namely (101),(102),(103), and (006) at 2θ equal to 27.64° , 29.24° , 31.3° , and 32.38° , respectively. These orientations indicate a covellite CuS phase with hexagonal structure. Whereas the presence of secondary phase of low chalcocite Cu_2S is also indicated from figure. The planes which corresponds to the above mentioned diffraction angles are closely corresponding to monoclinic structure along the (022),(202),(100),(-204),and (313), at 2θ equal to 21.08° , 23.50° , 25.66° , 26.2° and 36.22° , respectively. It is clear that there is a small peak related to cubic phase of CuS_2 along the (210) at 2θ equals 35.5° , as shown in table (1).

The results indicate that the CuS peaks displaced at higher 2θ , and Cu_2S peaks appears at lower 2θ .

The XRD pattern of $\text{Cu}_{1.75}\text{S}$ phase in fig.(1b) shows many peaks corresponds to (112), (211), (202), (113), (220), (004), (203), (104) planes at 2θ equal to 22.48° , 26.22° , 27.02° , 30.44° , 31.50° , 32.76° , 33.26° , and 34.16° respectively. These peaks confirm that the films belong to the orthorhombic structure, and there is a secondary phase with peaks for monoclinic phase of Cu_2S along (221) and (212) at 2θ equal to 23.18° and 24.40° , respectively.

The Fig.(1c) shows the XRD pattern of $\text{Cu}_{1.8}\text{S}$ phase has three peaks along the (555),(119),(0010) at 2θ equal to 27.18° , 29.48° , and 31.62° , respectively. These peaks related to cubic structure of Deginite structure, and five peaks exist as a secondary phase for $1.96 > x > 1.86$ hexagonal phase along the (121),(031),(220),(141) at 2θ equal to 19.0° , 20.18° , 22.94° and 30.36° , respectively.

The XRD pattern of $\text{Cu}_{1.95}\text{S}$ phase fig.(1d) has two peaks of cubic $\text{Cu}_{1.96}\text{S}$ phase along (111),(200) at 2θ equal to 27.08° and 31.58° , respectively. As well as, there is two peaks of hexagonal structure for $1.96 > x > 1.86$ phase along the (031), (131) at 2θ equal to 21.48° and 24.28° , respectively. The presence of secondary phase of Cu_2S peaks can be notes along (100),(-204) at 2θ equal 25.74° and 26.26° , respectively, and one peak for hexagonal $\text{Cu}_{1.92}\text{S}$ phase along (114) appear at 2θ equals 30.32° .

Fig.(1e) reveals the XRD pattern of Cu_2S phase which has six peaks for Cu_2S phase along (211),(022),(202),(212), (-223),(-114), at 2θ equal to 19.52° , 20.98° , 23.4° , 24.12° , 25.12° and 28.38 , respectively, this phase has monoclinic structure with preferred orientation along (-114) direction. All these result are shown in Table (1).

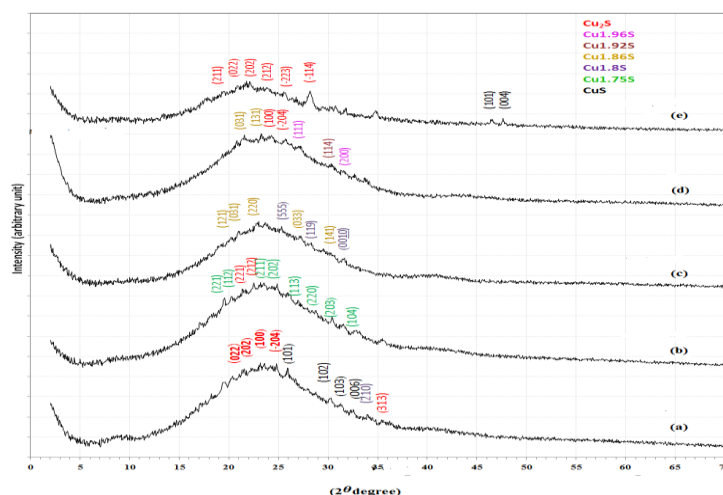


Fig. 1. Crystal structure of copper sulfide Cu_{2-x}S thin films with different molar ratio.
a- $x=1$ b- $x=0.25$ c- $x=0.20$ d- $x=0.05$ e- $x=0$.

The broad peaks observed refer to the reduced crystallite size of the prepared samples. A rough estimate of the average crystallite size by using the Scherrer formula gives a range of values (10-44.5) nm.

It is clear that the obtaining pure phase (one phase) is impossible thing because mixed phases are known in the moderate compositions. The copper sulfide compounds structure is complicated to a large degree. Even the structures of Cu_2S and CuS , which are supposed to be stoichiometric, are not consistent with their forming as Cu (I) and Cu (II) sulfides[22].

Table 1. Structural parameters viz. 2θ values, inter-planar spacing, miller indices, and crystallite size of Cu_{2-x}S films.

x	2θ (Deg.)	d_{hkl} Exp.(Å)	hkl	d_{hkl} Std.(Å)	FWHM (Deg.)	G.S (nm)	Phase	Card No.	
CuS	21.0800	4.2111	(022)	4.2390	0.5847	13.8	Cu_2S	33-490	
	23.5000	3.7826	(202)	3.7790	0.2765	29.4	Cu_2S	33-490	
	25.6600	3.4689	(100)	3.4210	0.3072	26.5	Cu_2S	24-57A	
	26.2000	3.3986	(-204)	3.3730	0.1849	44.1	Cu_2S	33-490	
	27.6400	3.2247	(101)	3.2230	0.1837	44.6	CuS	24-60	
	29.2400	3.0518	(102)	3.0500	0.2455	33.5	CuS	24-60	
	31.3000	2.8555	(103)	2.8150	0.4600	17.9	CuS	24-60	
	32.3800	2.7627	(006)	2.7270	0.5209	15.9	CuS	24-60	
	35.5000	2.5267	(210)	2.5266	0.4602	18.1	CuS_2	33-492	
	36.2200	2.4781	(313)	2.4780	0.3530	23.7	Cu_2S	33-490A	
Cu _{1.75} S	22.4800	3.9519	(112)	3.9280	0.3379	24.0	$\text{Cu}_{1.75}\text{S}$	33-489	
	23.1800	3.8341	(221)	3.8850	0.3984	20.4	Cu_2S	33-490	
	24.4000	3.6451	(212)	3.5990	0.7966	10.2	Cu_2S	33-490	
	26.2200	3.3961	(211)	3.3570	0.1849	44.1	$\text{Cu}_{1.75}\text{S}$	33-489	
	27.0200	3.2973	(202)	3.2180	0.1837	44.5	$\text{Cu}_{1.75}\text{S}$	33-489	
	30.4400	2.9342	(113)	3.0760	0.3066	26.9	$\text{Cu}_{1.75}\text{S}$	33-489	
	31.5000	2.8378	(220)	2.7800	0.4600	18.0	$\text{Cu}_{1.75}\text{S}$	33-489	
	32.7600	2.7315	(004)	2.7690	0.5209	15.9	$\text{Cu}_{1.75}\text{S}$	33-489	
	33.2600	2.6916	(203)	2.6990	0.4291	19.3	$\text{Cu}_{1.75}\text{S}$	33-489	
	34.1600	2.6227	(104)	2.6190	0.5514	15.1	$\text{Cu}_{1.75}\text{S}$	33-489	
Cu _{1.8} S	19.0000	4.6671	(121)	4.7500	0.5176	15.6	$x > 1.86$	23-958	
	20.1800	4.3968	(031)	4.2400	0.2749	29.4	$x > 1.86$	23-958	
	22.9400	3.8737	(220)	3.8800	0.4847	16.7	$x > 1.86$	23-958	
	27.1800	3.2783	(555)	3.2100	0.3634	22.5	$\text{Cu}_{1.8}\text{S}$	23-962	
	28.3200	3.1488	(033)	3.1600	0.3634	22.6	$x > 1.86$	23-958	
	29.4800	3.0275	(119)	3.0100	0.5455	15.1	$\text{Cu}_{1.8}\text{S}$	23-962	
	30.3600	2.9417	(141)	2.8600	0.6662	12.4	$x > 1.86$	23-958	
	31.6200	2.8273	(0010)	2.7790	0.4224	19.6	$\text{Cu}_{1.8}\text{S}$	23-962	
	21.4800	4.1336	(031)	4.2400	0.6343	12.8	$x > 1.86$	23-958	
	24.2800	3.6628	(131)	3.6000	0.1211	67.1	$x > 1.86$	23-958	
Cu _{1.95} S	25.7400	3.4583	(100)	3.4210	0.3928	20.8	Cu_2S	24-57A	
	26.2600	3.3910	(-204)	3.3700	0.2419	33.7	Cu_2S	33-490	
	27.0800	3.2901	(111)	3.3000	0.5138	15.9	$\text{Cu}_{1.96}\text{S}$	12-174	
	30.3200	2.9455	(114)	2.9200	0.4835	17.0	$\text{Cu}_{1.92}\text{S}$	30-505	
	31.5800	2.8308	(200)	2.8500	0.4230	19.5	$\text{Cu}_{1.96}\text{S}$	12-174	
	Cu ₂ S	19.5200	4.5440	(211)	4.6680	0.2820	28.6	Cu_2S	33-490
		20.9800	4.2309	(022)	4.2390	0.2740	29.5	Cu_2S	33-490
23.4000		3.7986	(202)	3.779	0.3140	25.8	Cu_2S	33-490	
24.1200		3.6868	(212)	3.5990	0.5600	14.5	Cu_2S	33-490	
25.1200		3.5422	(-223)	3.5500	0.4040	20.2	Cu_2S	33-490	
28.3800		3.1423	(-114)	3.1580	0.5812	14.1	Cu_2S	33-490	

Atomic force microscopy (AFM) is one of the most effective ways for the surface analysis due to its high resolution and powerful analysis. The knowledge of the surface topography at nanometric resolution made possible to probe thin film surfaces. The versatility of this technique

allows meticulous observations and evaluations of the textural and morphological characteristics of the films, showing better facilities than other microscopic methods.

Fig.2 shows the three and two dimensional AFM images of Cu_{2-x}S thin films for different molar ratio, by scanned the surface in 3D and the analysis of the images allow the determination of the average height of the particles, the root mean square roughness and the periodicity in the arrangement of particles. It is possible to evaluate characteristics such as roughness, porosity, average size, and particle size distribution, which influence directly the optical, surface, and electrical properties of thin films.

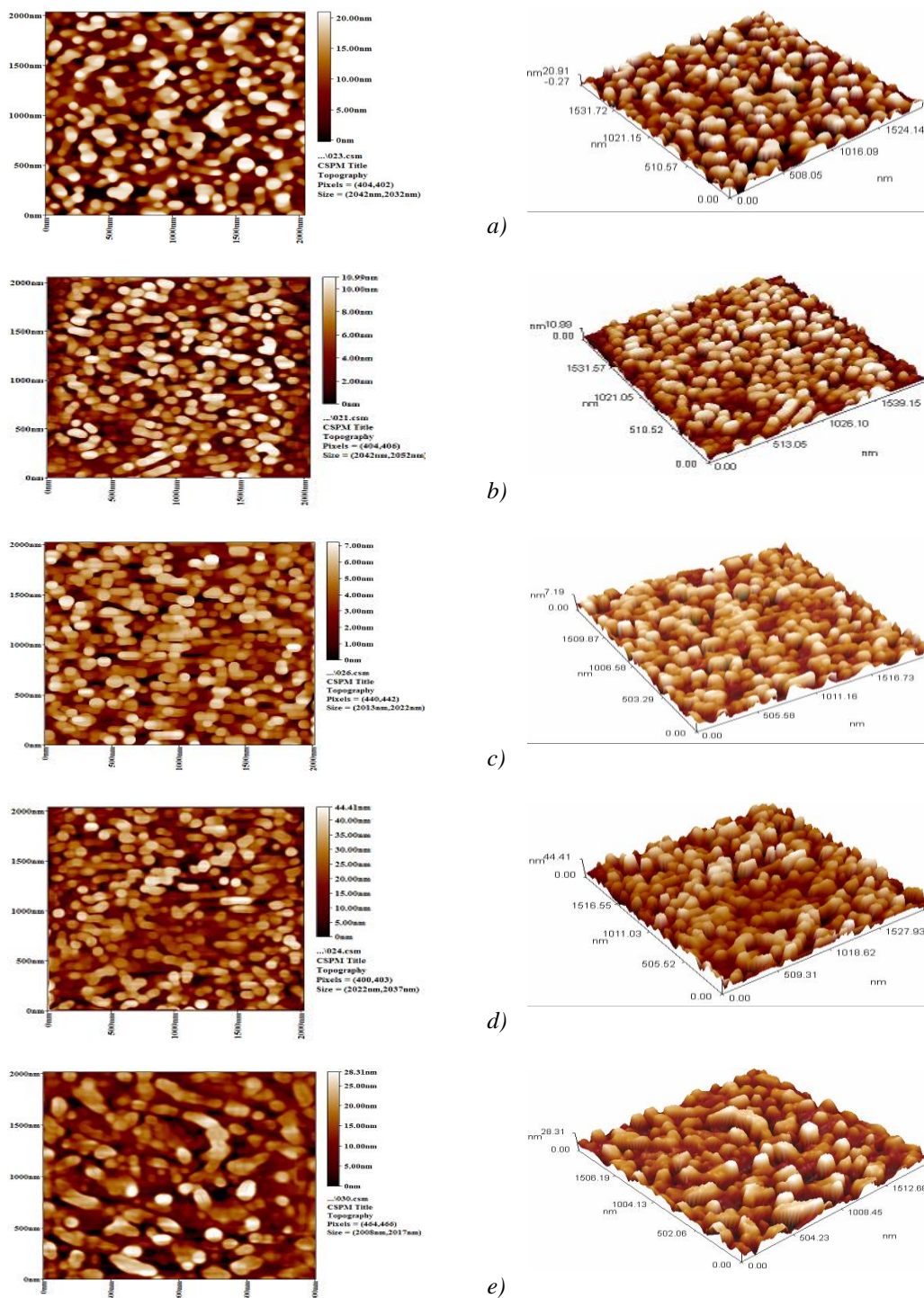


Fig. 2. 2D and 3D images of Cu_{2-x}S thin films with different molar ratio.
 a- $x=1$ b- $x=0.25$ c- $x=0.20$ d- $x=0.05$ e- $x=0$.

Its clear from the images that the films are uniform, without cracks and consists of nanosize particles which are well adhered to the substrate. The morphology was first spherical for CuS film ($x=1$), and then changed to tetragonal and granular with decreasing x to 0.25 and 0.20. It is obvious that the particles tend to be rod like which can be evident from con shape, spiky structure for $x=0.05$ and $x=0$ as shown in fig.(2 d&e).

AFM studies shows that the average diameter has maximum value of 98.0 nm for Cu_2S and minimum value of 72.22 nm for $\text{Cu}_{1.75}\text{S}$. The Root Mean Square (RMS) roughness which is defined as the standard deviation of the surface height profile from the average height is the most commonly reported measurement of surface roughness. The RMS roughness calculates the standard deviation of the surface irregularities with respect to some mean line or curve. It is commonly used to characterize optical components, in general the lower the RMS value, the less light is scattered by an optical surface, and hence the better the surface quality [5]. The change of surface roughness is due to the crystallite size variation, and average roughness with maximum value of 8.21nm for $\text{Cu}_{1.95}\text{S}$ and minimum value of 1.32 nm for $\text{Cu}_{1.80}\text{S}$, and maximum value of root mean square equal to 9.83 nm for $\text{Cu}_{1.95}\text{S}$ and minimum value for $\text{Cu}_{1.8}\text{S}$ equal to 1.6 nm. Table (2) illustrated all parameter which obtained from surface morphology study.

Table2. Average diameter of grains, surface roughness, RMS roughness, and height of Cu_{2-x}S thin films.

Molar ratio	Average diameter(nm)	Average roughness (nm)	Root mean square(Sq) (nm)	Height (nm)
1.00	90.00	5.29	6.08	20.91
1.75	72.22	2.48	2.90	10.99
1.80	97.53	1.32	1.60	7.19
1.95	81.08	8.21	9.83	44.41
2.00	98.00	5.46	6.56	28.31

The optical properties of deposited Cu_{2-x}S with different molar ratios on glass substrates by chemical bath deposition method have been studied by measuring transmission and absorption in the wavelength range (300-1100) nm .

Optical transmittance spectra of the Cu_{2-x}S films displayed in figure (3) which shows that the films transmit well in the end of visible and NIR region of the solar spectrum (600-1100) nm, where the transmittance increases with increase wavelength and then remained constant. The films exhibit high transparency that, in most cases exceeds 70% in the NIR region. This high transparency related to low thickness of the films, this is mention by Dhondge and Kirmizigul et al [5,19]. It is clear that the transmittance increased with increasing the molar ratio ,where it reach to maximum value (90%) for $x=1.80$.

The variation of absorption coefficient with wavelength for Cu_{2-x}S thin films is shown in figure (4) The absorption edge gets shifted toward the shorter wavelength with increasing the molar ratio . In the chemical bath deposition synthesized thin films, the strong absorption is in the wavelength range 325 nm to 600 nm , and this is agree with Chaki et al.[21]. The a broad absorption between 350 and 600 nm for these films is the most important reason for their applications in solar energy adsorption and photovoltaic devices, also the high absorbance in the UV region and low absorbance in the visible region have useful application in the coating of windscreens and driving mirrors to prevent the effect of the dazzling light into drivers eyes from oncoming and following vehicles.

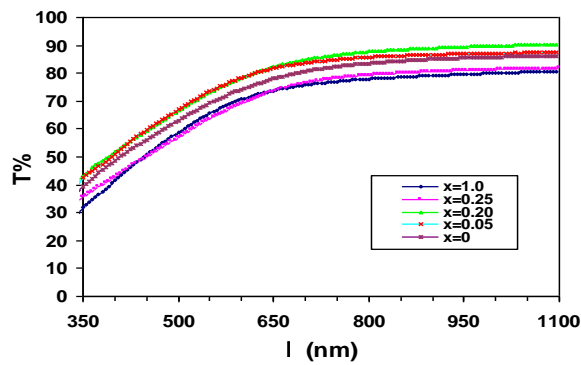


Fig. 3. Transmittance vs. wavelength of $u_{2-x}S$ thin films with different molar ratio.

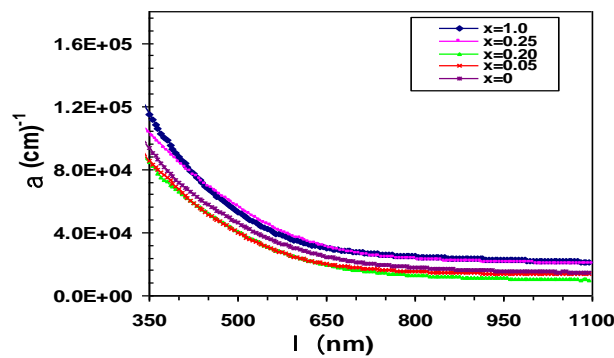


Fig. 4. The relation between the a and wavelength of $Cu_{2-x}S$ thin films with different molar ratio.

The optical band gap energy of the semiconductor is an important parameter that plays a major role in the construction of photovoltaic cells.

CuS is considered as a direct band gap semiconductor, so the relationship between the adsorption coefficient (α) near the absorption edge and the optical band gap (E_g) for direct band transitions obeys Taucs relation [8]:

$$(\alpha h\nu)^2 = B(h\nu - E_g) \quad (1)$$

Where $h\nu$ is photon energy and B is a constant. Fig. 5 shows the graphs of $(\alpha h\nu)^2$ vs. photon energy ($h\nu$) indicates that the CuS films are essentially direct-transition-type semiconductors. The straight-line portion of the curve, when extrapolated to zero, gives the optical band gap E_g . The E_g was increase from 2.78 eV for CuS to maximum value (3 eV) at molar ratio equal to 1.8 and then decreases to 2.9 eV with more increasing in the molar ratio. This variation in the energy gap occur due to the changing in the structure of the films with different molar ratio, where the absorption in the short wavelength side corresponds to that of chalcocite phase, and that of absorptions at long wavelength related to that of the covellite phase of copper sulphide and this is agree with Sangma and Kalita [23]. The reported value of direct band gap ranges from 2.1-2.8 eV for CuS thin film deposited by various methods [18,24].

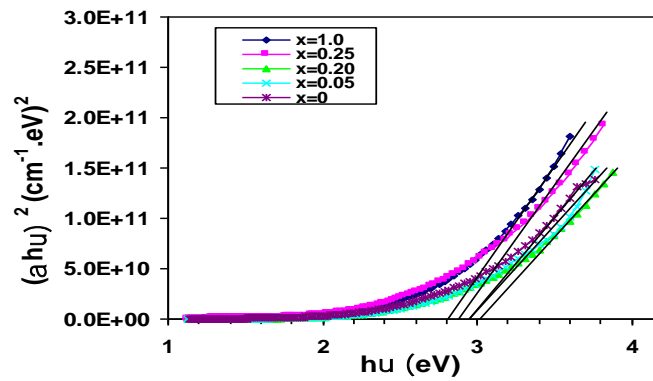


Fig. (5) $(ahv)^2$ vs. (hv) plots of $Cu_{2-x}S$ thin films with different molar ratio.

The refractive index (n) as a function of wavelength of $Cu_{2-x}S$ thin films for different molar ratio was shown in Fig. (6). The refractive index generally decreases with increase wavelength and also it reduces with increase the molar ratio and return to increase slightly for Cu_2S film. This means the CuS film have higher refractive index compared with the other samples. Fig. (7) display the relation between the extinction coefficient (k) and wavelength for $Cu_{2-x}S$ thin films. It is obvious that the extinction coefficient take the similar behavior of corresponding absorption coefficient, it is decrease from 0.158 for CuS to 0.083 for $Cu_{1.80}S$ film and then increase slightly to 0.114 with increasing the molar ratio to 2.

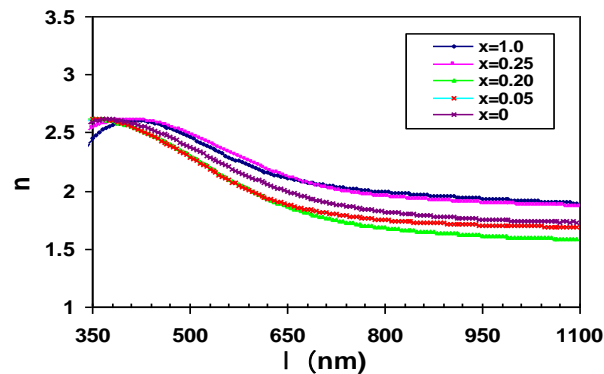


Fig. (6) The refractive index vs. the wavelength of $Cu_{2-x}S$ thin films with different molar ratio

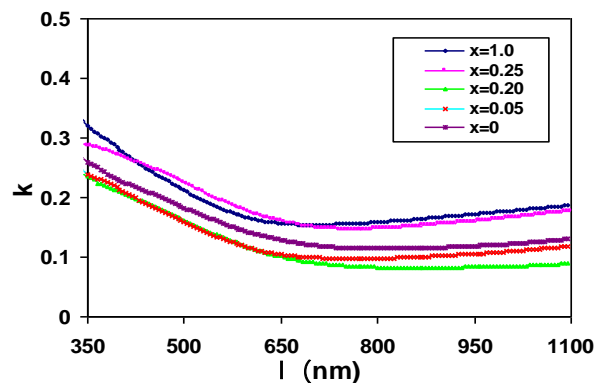


Fig. (7) The extinction coefficient vs. the wavelength Of $Cu_{2-x}S$ thin films with different molar ratio

The real (ϵ_r) and imaginary (ϵ_i) parts of dielectric constant were also determined. The behavior of ϵ_r similar to refractive index because the smaller value of k^2 comparison of n^2 , while ϵ_i is mainly depends on the k values, which are related to the variation of absorption coefficient. In general the dielectric constants decrease with increasing molar ratio.

The optical properties parameters including , energy gap, absorption coefficient, refractive index, extinction coefficient , real and imaginary part of the dielectric constant at wavelength equals to 800 nm of Cu_{2-x}S thin films are listed in table (3).

Table3.The optical constants of Cu_{2-x}S thin films for different molar ratio, at $\lambda=800$ nm.

Molar ratio	$E_g^{\text{opt}}(\text{eV})$	$\alpha(\text{cm}^{-1}) \cdot 10^4$	n	k	ϵ_r	ϵ_i
1.00	2.78	2.49	1.990	0.158	3.938	0.631
1.75	2.86	2.32	1.952	0.147	3.790	0.577
1.80	3.00	1.31	1.683	0.083	2.827	0.280
1.95	2.92	1.54	1.750	0.097	3.055	0.342
2.00	2.90	1.80	1.822	0.114	3.307	0.416

The type of charge carriers, conductivity, carriers concentration (n_H) and Hall mobility (μ_H), have been estimated from Hall measurements. Table (4) illustrates the main parameters estimated from Hall Effect measurements of Cu_{2-x}S thin films for different molar on glass substrates. It is clear from this table that all Cu_{2-x}S thin films have a positive Hall coefficient (p-type).The conductivity increase from 0.246×10^{-3} to $2.4 \times 10^{-1} (\Omega \cdot \text{cm})^{-1}$ with increasing the molar ratio to 1.80 and then decreases to $2.10 \times 10^{-2} (\Omega \cdot \text{cm})^{-1}$. In general the carrier concentration increases with increasing molar ratio except for $\text{Cu}_{1.8}\text{S}$ which has a lower values of carrier concentration and holes mobility . Cu_2S thin film is the best because it has the highest carrier concentration $1.0 \times 10^{15} \text{ cm}^{-3}$ and mobility ($5740 \text{ cm}^2/\text{V} \cdot \text{s}$) and good conductivity which make the thin film very good for device performance as shown in table (4).

Table 4. The electrical measurements of Cu_{2-x}S thin films for different molar ratio

Molar ratio	Type	$\sigma \times 10^{-3} (\Omega \cdot \text{cm})^{-1}$	$n \times 10^{13} (1/\text{cm}^3)$	μ (cm/V.s)
1.00	p-type	0.246	0.668	229.9
1.75	p-type	927.0	74.19	2049
1.80	p-type	240.0	2.518	134.2
1.95	p-type	0.541	34.02	385.6
2.00	p-type	21.00	100.9	5740

4. Conclusions

This study revealed the effect of molar ratio of precursors on the structural, morphological, optical, and electrical properties of Cu_{2-x}S thin films fabricated on a glass substrate by chemical bath deposition method. The structure of Cu_{2-x}S films was amorphous with small peaks related to different phases. Surface morphology reveals uniform surface without cracks and consists of nanosize particles which are well adhered to the substrate.

The optical transmittance of Cu_{2-x}S films increases with increasing the molar ratio of Cu, and it had high values in near IR region because the thickness of the films was very thin. The absorbance of these films observed in the range 350-600 nm. These properties make the Cu_{2-x}S films suitable for solar control coating and photovoltaic devices.

References

- [1] R.Suja, D.Geetha, P.Ramesh, International Journal of Scientific & Engineering Research **4**(3), 1(2013).
- [2] J. C. Osuwa, E. C. Mgbaja, IOSR Journal of Applied Physics **6**(5), 28 (2014).
- [3] Yong-Juan Lu, Jun-Hong Jia, Chinese Chemical Letters **25**,1473(2014).
- [4] Singh A. Kumar, Mehra Swati, Thool G. Sheel, Austin Chem. Eng. **1**(1),1 (2014).
- [5] Ajaya K. Singh, Swati Mehra, Gautam S. Thool, European Chemical Bulletin **2**(8),518 (2013).
- [6] A. D. Dhondge, S. R. Gosavi, N. M. Gosavi, C. P. Sawant, A. M. Patil, A. R. Shelke, N. G. Deshpande, World Journal of Condensed Matter Physics **5**,1 (2015).
- [7] Joyjit Kundu, Debabrata Pradhan, New J. Chem. **37**, 1470 (2013).
- [8] H. Y. He, Optoelectron. Adv. Mat. **5**(12), 1301 (2011).
- [9] I. A. Ezenwa, C. I. Elekalachi, International Journal of Materials Chemistry and Physics **1**(3), 281 (2015).
- [10] M. Annie Freeda, C. K. Mahadevan, S. Ramalingom, Archives of Physics Research **2**(3), 175 (2011).
- [11] L. A. Isac, A. Duta, A. Kriza, I. A. Enesca, M. Nanu, Journal of Physics: Conference Series, **61**,477 (2007).
- [12] Jiban Podder, Ryohei Kobayashi, Masaya Ichimura, Thin Solid Films **472**,71 (2005).
- [13] Satoshi Kurumi, Yohei Shimizu, Shotaro Kobayashi, Kouichi Takase, Kaoru Suzuki, Appl. Phys A **93**,741 (2008).
- [14] Johanna Johansson, Juhana Kostamo, Maarit Karppinen, Lauri Niinisto, J. Mater. Chem. **12**,1022 (2002).
- [15] Sohail Saeed, Naghmana Rashid, Khuram Shahzad Ahmed, Turk J Chem **37**,796 (2013).
- [16] Aykut Astam, Yunus Akaltun, Muhammet Yildirim, Turk J Phys **38**,245 (2014).
- [17] S.S. Dhasade, J.S. Patil, J.V. Thombare, V. J. Fulari, J. of Shivaji University (Science & Technology) **41**(2),1 (2015).
- [18] M. Dhanasekar, G. Bakiyaraj, K. Rammurthi, International Journal of Chem Tech Research **7**(3), 1057 (2015).
- [19] F. Kirmizigul, E. Guneri, F. Gode, C. Gumus, Chalcogenide Letters **10**(5), 173 (2013).
- [20] I. A. Ezenwa, Res. J. Engineering Sci. **2**(1),1 (2013).
- [21] Sunil H. Chaki, M.P. Deshpande, Jiten P. Tailor, Thin Solid Films **550**, 291 (2014).
- [22] Fayroz A. Sabah, Naser M. Ahmed, Z. Hassan, Hiba S. Rasheed, Journal of Scientific Research and Development **2**(13),95 (2015).
- [23] Alaric D. Sangma, P. K. Kalita, International Journal of Chemical Science and Technology **2**(4), 57 (2012).
- [24] B. Guzeldir, M. Saglam, A. Ates, Acta Phys. A. **121**, 33 (2012).